IAI Journals.ASM.org

Killer Cell Lectin-Like Receptor G1 Deficiency Significantly Enhances Survival after *Mycobacterium tuberculosis* Infection

Joshua C. Cyktor,[a,b] Bridget Carruthers,[b] Paul Stromberg,[c] Emilio Flaño,[b,d] Hanspeter Pircher,[e] Joanne Turner[a,b]

Department of Microbial Infection and Immunity, The Ohio State University, Columbus, Ohio, USA[a]; Center for Microbial Interface Biology, The Ohio State University, Columbus, Ohio, USA[b]; Department of Veterinary Biosciences, The Ohio State University, Columbus, Ohio, USA[c]; Center for Vaccines and Immunity, The Research Institute at Nationwide Children's Hospital, Columbus, Ohio, USA[d]; Department of Immunology, Institute of Medical Microbiology and Hygiene, University of Freiburg, Freiburg, Germany[e]

The expression of T cell differentiation markers is known to increase during *Mycobacterium tuberculosis* infection, and yet the biological role of such markers remains unclear. We examined the requirement of the T cell differentiation marker killer cell lectin-like receptor G1 (KLRG1) during *M. tuberculosis* infection using mice deficient in KLRG1. KLRG1$^{-/-}$ mice had a significant survival extension after *M. tuberculosis* infection compared to wild-type controls, and maintained a significantly lower level of pulmonary *M. tuberculosis* throughout chronic infection. Improved control of *M. tuberculosis* infection was associated with an increased number of activated pulmonary CD4$^+$ T cells capable of secreting gamma interferon (IFN-γ). Our report is the first to show an *in vivo* impact of KLRG1 on disease control.

Killer cell lectin-like receptor G1 (KLRG1) expression identifies natural killer (NK) cells and antigen-experienced T cells that have become terminally differentiated (1–3). Unlike some NK receptors, KLRG1 binds to nonclassical major histocompatibility complex (MHC) molecules of the cadherin family (E-, N-, and R-cadherin) (4, 5). While the structure (6) and ligands of KLRG1 are known, the biological function of KLRG1 *in vivo* is still unclear. The majority of our current understanding of KLRG1 is derived from *in vitro* studies, which demonstrated that KLRG1 ligation can negatively affect the functional activity of NK and CD8$^+$ T cells (4, 5, 7–11). Despite this, NK and CD8$^+$ T cell responses in several infection models were normal in KLRG1-deficient mice (7). In addition, an inhibitory function of KLRG1 in *ex vivo*-isolated NK cells was observed only in transgenic mice overexpressing KLRG1 (7).

The expression of KLRG1 on T cells increases during *M. tuberculosis* infection and decreases after chemotherapy (12), suggesting a correlation between KLRG1 expression and disease progression. Studies using adoptive transfer of KLRG1$^+$ T cells determined that, during *M. tuberculosis* infection, KLRG1$^+$ effector cells were capable of gamma interferon (IFN-γ) production but impaired in their proliferative capacity (13). This finding supported the hypothesis that KLRG1 marks terminally differentiated cells, but the *in vivo* functional kinetics and biological impact for KLRG1 expression during *M. tuberculosis* infection are still unclear. In this report, we demonstrate for the first time that C57BL/6 mice deficient in KLRG1 had a highly significant survival advantage over wild-type mice and that the advantage was associated with reduced *M. tuberculosis* burden during chronic infection. Although the majority of studies in viral infection suggests that KLRG1 expression impacts NK and CD8$^+$ T cell function (11, 14), we observed no differences in CD8$^+$ T cell numbers or function, instead finding a significant increase in pulmonary CD4$^+$ T cell numbers as well as production of IFN-γ and tumor necrosis factor (TNF) within the CD4$^+$ T cell population. Our studies demonstrate an *in vivo* biological relevance of KLRG1 expression in an infection model that was highly associated with enhanced CD4$^+$ T cell function and long-term control of *M. tuberculosis* infection.

MATERIALS AND METHODS

Mice. Specific pathogen-free, age- and sex-matched C57BL/6 KLRG1$^{-/-}$ mice (7) and C57BL/6 wild-type mice (The Jackson Laboratory, Bar Harbor, ME) were maintained in ventilated cages inside a biosafety level 3 (BSL3) facility and provided with sterile food and water *ad libitum*. All protocols were approved by The Ohio State University's Institutional Laboratory Animal Care and Use Committee. Control hybrid mice were created by crossing KLRG1$^{-/-}$ animals with C57BL/6 wild-type mice (The Jackson Laboratory). The heterozygous (+/−) offspring were crossed with homozygous (−/−) knockout mice to generate KLRG1$^{+/-}$ and KLRG1$^{-/-}$ mice, which were subsequently infected with *M. tuberculosis* and analyzed for CFU at day 120 postinfection. The genotype of these mice was identified on splenic cells by flow cytometry using KLRG1-specific antibodies at necropsy.

***M. tuberculosis* infection and CFU enumeration.** *M. tuberculosis* Erdman (ATCC no. 35801) was obtained from the American Type Culture Collection. Stocks were grown according to published methods (15). Mice were infected with *M. tuberculosis* Erdman using an inhalation exposure system (Glas-Col) calibrated to deliver 50 to 100 CFU to the lungs of each mouse, as previously described (15). At specific time points post-*M. tuberculosis* infection, mice were sacrificed and lungs and spleens were aseptically removed into sterile saline solution. Organs were homogenized and serial dilutions plated onto 7H11 agar supplemented with oleic acid-albumin-dextrose-catalase (OADC) as previously described (16). Plates were incubated at 37°C for 21 days in order to enumerate bacterial colonies and calculate the bacterial burden.

Survival studies. Groups of wild-type and KLRG1$^{-/-}$ C57BL/6 mice were infected with *M. tuberculosis* Erdman via aerosol and maintained in a BSL3 facility (17). Mice were observed daily and euthanized when moribund, and the date of euthanasia was recorded. Survival studies were

Received 31 October 2012 Returned for modification 27 November 2012
Accepted 11 January 2013
Published ahead of print 22 January 2013
Editor: J. L. Flynn
Address correspondence to Joanne Turner, joanne.turner@osumc.edu.

doi:10.1128/IAI.01199-12

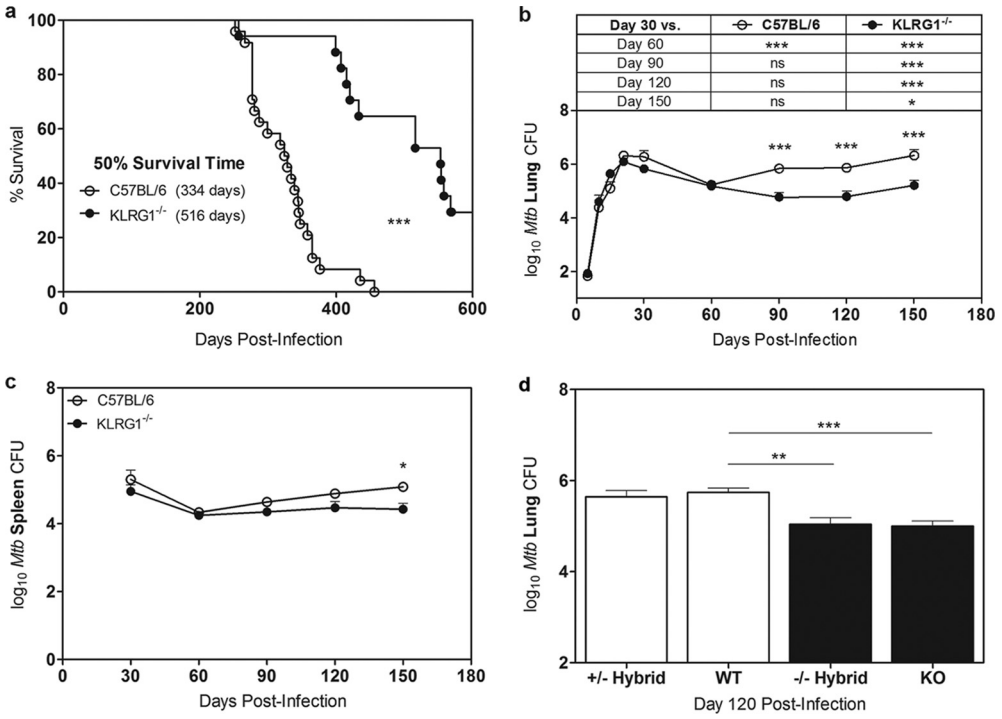

FIG 1 Survival of wild-type or KLRG1$^{-/-}$ C57BL/6 mice and *M. tuberculosis* burden. Wild-type and KLRG1$^{-/-}$ C57BL/6 mice were infected with *M. tuberculosis* (*Mtb*). (a) Survival time. Mice were maintained under BSL3 conditions, monitored daily, and euthanized when moribund ($n = 25$ wild type, 25 KLRG1$^{-/-}$). (b and c) Subsets of infected mice were sacrificed at various time points postinfection and lungs (b) and spleens (c) removed for CFU enumeration on 7H11 plates. (b) Top: table comparing day 30 to other time points within the same group by two-way ANOVA. Data are representative of the results of two independent experiments with 5 mice per group per time point. (d) Pulmonary *M. tuberculosis* CFU from wild-type (WT) or KLRG1$^{-/-}$ (KO) C57BL/6 mice versus heterozygous crosses at day 120 postinfection. Data are representative of the results of one experiment with 10 mice per group. *, $P < 0.05$; **, $P < 0.01$; ***, $P < 0.001$ (as obtained by Student's *t* test for comparisons between groups). Survival significance was determined by a log rank Mantel-Cox test.

performed twice ($n = 25$ wild-type and 25 KLRG1$^{-/-}$ mice or 30 wild-type and 25 KLRG1$^{-/-}$ mice).

Lung cell isolation. Mice were euthanized by CO_2 asphyxiation, and lungs were perfused through the right ventricle with cold phosphate-buffered saline containing 50 U/ml of heparin. Lungs from individual mice were mechanically disrupted using a GentleMACS dissociator (Miltenyi Biotec, Boston, MA) followed by collagenase A (type XI) (Sigma) (0.7 mg/ml) and type IV (Sigma) (30 μg/ml) bovine pancreatic DNase diges-

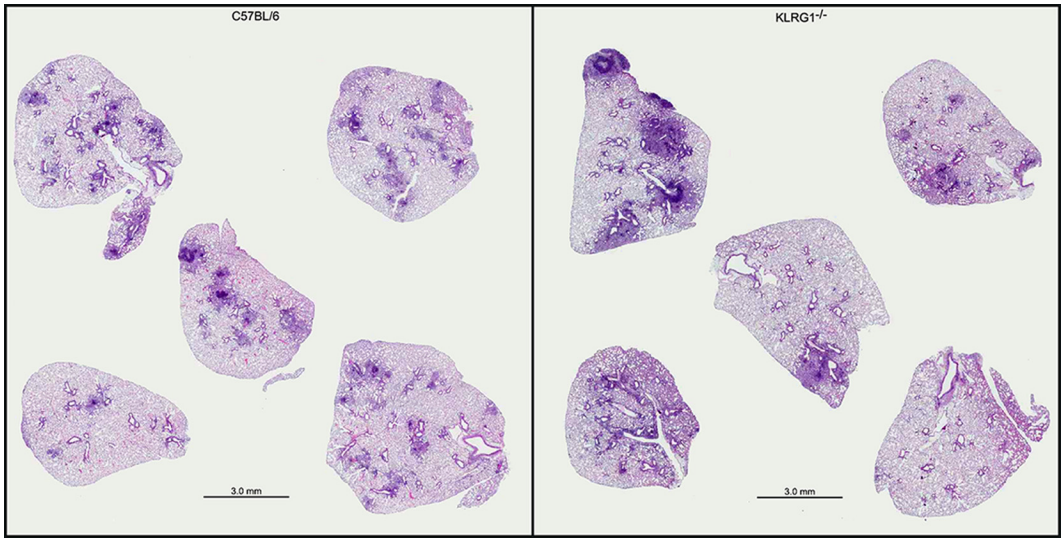

FIG 2 Pulmonary histology of KLRG1$^{-/-}$ mice. Wild-type and KLRG1$^{-/-}$ C57BL/6 mice were infected with *M. tuberculosis*. At day 90 postinfection, groups of mice were sacrificed and lungs removed and fixed in formalin for histological analysis. Images representative of lung lobes from 5 mice at day 90 postinfection stained with hematoxylin and eosin are shown.

TABLE 1 Microscopic lung lesions from *M. tuberculosis*-infected mice

Day	Characterization[a]	
	C57BL/6	KLRG1$^{-/-}$
90	Mild multifocal areas of unorganized granulomatous inflammation; irregular lymphoid aggregates around small airways; no necrosis or caseation; few AFB are present	Mild multifocal areas of unorganized granulomatous inflammation; typical epithelioid Mφ are present with fewer foamy Mφ and small aggregates of PMN and pyknotic debris; no AFB are observed
120	Moderate to mild multifocal to coalescing granulomatous inflammation; epithelioid and foamy Mφ are present with foci of lymphocytic nodules often around small vessels and airways; few AFB are present, distributed as attenuated individual bacteria in Mφ	Mild multifocal unorganized granulomatous foci with epithelioid and foamy Mφ; lymphoid cuffs are present around many adjacent small airways and vessels; there are a few aggregates of PMN in the foci, but there is little pyknosis; very few isolated individual attenuated AFB are noted in the foamy Mφ
150	Coalescing areas of granulomatous inflammation; cells are predominately epithelioid and foamy Mφ with scattered PMN; no overall caseation necrosis; alveolar septae are thickened; few AFB are visible, appearing as single isolated attenuated rods in Mφ	Moderate multifocal areas of unorganized granulomatous inflammation; some coalescing foci, but many are small, individual, and populated by typical granulomatous exudate; epithelioid and foamy Mφ with a few scattered aggregates of PMN and pyknotic debris; very few AFB present
220	Extensive multifocal to coalescing foci of unorganized granulomatous inflammation; predominately epithelioid and foamy Mφ are present, punctuated by small aggregates of lymphocytes and PMN; cholesterol clefts are noted in some of the confluent foci; some bronchioles have degenerate PMN, foamy Mφ, and pyknotic debris in the lumen; few visible AFB	Extensive multifocal to coalescing unorganized inflammation; primarily epithelioid and foamy Mφ, some with degenerative changes but little pyknosis; occasional cholesterol clefts are noted; typical lymphoid aggregates are present around small airways and vessels; few AFB are present and are distributed as attenuated rods in foamy Mφ

[a] Mφ, macrophage; PMN, polymorphonuclear cell; AFB, acid-fast bacilli.

tion at 37°C for 30 min in GentleMACS C-tubes. Lung cell suspensions were passed through a 70-μm-pore-size nylon cell screen, and residual erythrocytes were lysed with Gey's solution. Viable cells were determined by trypan blue exclusion.

Cell purification. Single lung cell suspensions were adhered to sterile tissue culture dishes for 1 h at 37°C. Nonadherent cells were washed and removed from the plates. CD4$^+$ T cells were obtained from the nonadherent cell fraction by magnetic cell separation (BD IMag anti-CD4 particles, clone GK1.5) (BD Biosciences, San Jose, CA). The purity of the CD4$^+$ T cell populations was determined to be greater than 90% for all experiments by flow cytometry using an LSRII flow cytometer (BD Biosciences).

Cytokine assays. Purified pulmonary CD4$^+$ T cells (1×10^5) were cultured with *M. tuberculosis* culture filtrate protein (CFP) (BEI Resources, NIAID, NIH) for 48 h at 37°C with 5% CO_2. After incubation, plates were frozen at −80°C until all time points were completed. IFN-γ enzyme-linked immunosorbent assay (ELISA) antibodies and standards were obtained from BD Biosciences and processed as previously described (15). Levels of TNF in cell supernatants were determined using a mouse TNF ELISA Ready-SET-Go! kit from Ebioscience (San Diego, CA) according to the manufacturer's instructions. Colormetric reactions were read on a SpectraMax plate reader (Molecular Devices, Sunnyvale, CA).

Flow cytometry. Isolated lung cells were suspended in deficient RPMI medium (Sigma) supplemented with 0.1% sodium azide (Sigma). Surface targets were detected as previously described (18). The following specific antibodies and isotype controls were purchased from BD Biosciences: peridinin chlorophyll protein (PerCP)-Cy5.5 anti-CD3 (145-2C11), allophycocyanin (APC)-Cy7 anti-CD3 (17A2), PerCP-Cy5.5 anti-CD11b (M1/70), phycoerythrin (PE) anti-FoxP3 (MF23), PE anti-NK1.1 (PK136), APC-Cy7 anti-CD4 (GK1.5), PE-Cy7 anti-CD8 (53-6.7), PerCP-Cy5.5 anti-CD8 (53-6.7), PE-Cy7 anti-IFN-γ (XMG1.2), PE anti-TNF (MP6-XT22), and PE anti-CD69 (H1.2F3). FoxP3 buffer set (BD Biosciences), PE or APC anti-KLRG1 (2F1), APC anti-perforin (eBioO-MAK-D), and PE anti-granzyme B (NGZB) antibodies were purchased from eBiosciences. Cytokine levels and perforin/granzyme B degranulation were determined according to the manufacturer's instructions for intracellular staining (Cytofix/Cytoperm fixation/permeabilization solution kit with BD GolgiStop; BD Biosciences). Cytokines were stained following a 4-h incubation with 10 μg/ml anti-CD3 (145-2C11) and 1 μg/ml anti-CD28 (37.51) in the presence of GolgiStop or concanavalin A (ConA; Sigma) (10 μg/ml) and GolgiStop. Mice were injected with bromodeoxyuridine (BrdU) 24 h prior to necropsy, and intracellular BrdU was quantified using a BD fluorescein isothiocyanate (FITC) BrdU kit (BD Biosciences) as described previously (19). Samples were read using an LSRII flow cytometer and analyzed with FACSDiva software (BD Biosciences). Lymphocytes were gated into CD3$^+$ CD4$^+$ T cells and CD3$^+$ CD8$^+$ T cells, with or without KLRG1.

Histology. Caudal lung lobes were taken from infected wild-type and KLRG1$^{-/-}$ C57BL/6 mice at various time points postinfection, inflated, and stored in formalin as previously described (20). Tissue sections were prepared and stained with hematoxylin and eosin or Ziehl-Neelsen stain and were assessed by a board-certified veterinary pathologist with no prior knowledge of the experimental groups.

Statistics. Statistical analysis was performed with GraphPad Prism software using the Student *t* test for comparisons between groups of mice per individual time point of each graph. All comparisons between time points of the same group utilized a two-way analysis of variance (ANOVA) test with Bonferonni posttests for multiple comparisons. Survival significance was determined by a log rank Mantel-Cox test.

RESULTS

KLRG1 deficiency significantly extends survival after *M. tuberculosis* infection. In contrast to the lack of a phenotype that has been observed in viral models of KLRG1 deficiency (7), KLRG1$^{-/-}$ mice infected with *M. tuberculosis* via the respiratory route had significantly extended survival compared to wild-type C57BL/6 mice (Fig. 1a). KLRG1$^{-/-}$ mice survived beyond day 600 in two independent experiments, while C57BL/6 mice had a median survival time of 334 days, which was within the expected range for this strain (21). Time to 50% survival was 334 days for wild-type mice and 516 days for KLRG1$^{-/-}$ mice, an approximately 35% increase in survival (Fig. 1a). Initial lung CFU numbers were equivalent, but KLRG1$^{-/-}$ mice were able to stabilize pulmonary *M. tuberculosis* burden with 1 log fewer CFU than

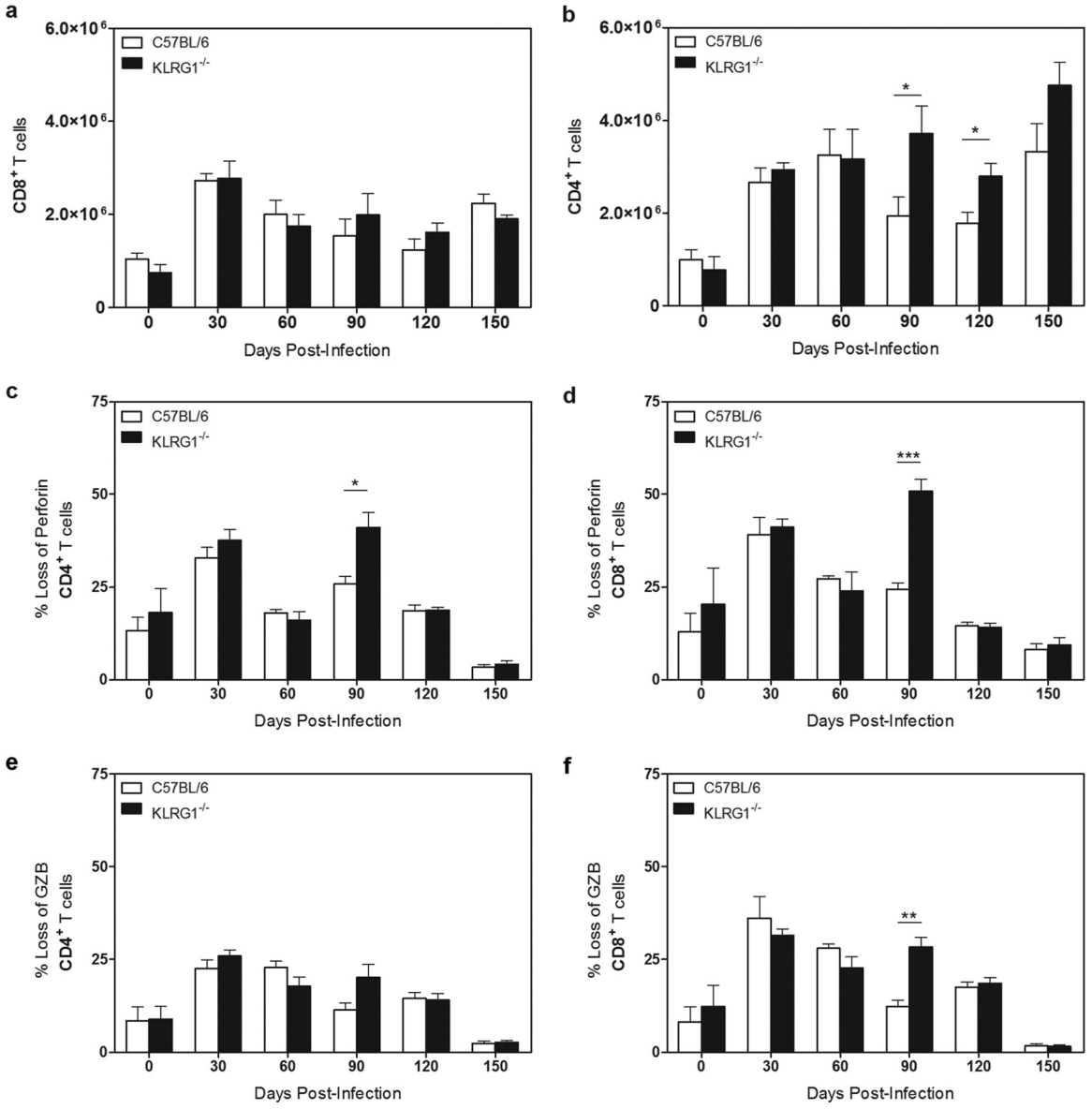

FIG 3 Pulmonary T cell composition and cytotoxic response of KLRG1$^{-/-}$ mice. Wild-type and KLRG1$^{-/-}$ C57BL/6 mice were infected with *M. tuberculosis*. At various time points postinfection, groups of mice were sacrificed and lungs removed and processed for analysis by flow cytometry. (a and b) Absolute numbers of CD8$^+$ T cells (a) and CD4$^+$ T cells (b) as determined by flow cytometry. (c to f) Percent loss of perforin in CD4$^+$ (c) or CD8$^+$ (d) T cells or of granzyme B (GZB) in CD4$^+$ (e) or CD8$^+$ (f) T cells. Degranulation is represented as percent loss of perforin and granzyme B (GZB) determined by subtracting values representing the remaining perforin/GZB expression from 100. Data are representative of the results of two independent experiments with 5 mice per group per time point. *, $P < 0.05$; **, $P < 0.01$; ***, $P < 0.001$ (as obtained by Student's *t* test).

wild-type mice from day 60 onward after infection (Fig. 1b). Relative to pulmonary CFU at day 30 postinfection, KLRG1$^{-/-}$ mice were able to sustain significantly lower *M. tuberculosis* CFU throughout infection, in contrast to the moderate regrowth of *M. tuberculosis* in the lungs of wild-type C57BL/6 mice that has also been reported by others (22, 23). The pulmonary *M. tuberculosis* burden before day 21 was not significantly different between groups, suggesting that KLRG1 does not affect innate immune responses sufficiently to impact *M. tuberculosis* CFU (Fig. 1b). Histological analysis of *M. tuberculosis*-infected lung tissue showed that KLRG1$^{-/-}$ mice did not have altered lung granulomas compared to wild-type mice (Fig. 2, Table 1), indicating that KLRG1 deficiency does not affect the recruitment or organization of T cells around infected macrophages.

A subset of KLRG1$^{-/-}$ mice from the survival study were euthanized at day 365 and at day 630 of infection, and the *M. tuberculosis* burden was found to have increased to 6.228 ($\pm$0.49, $n = 5$) log and 6.4 ($\pm$0.19, $n = 9$) log, respectively (not shown). Therefore, KLRG1$^{-/-}$ mice showed some evidence of moderate disease progression (increased pulmonary CFU) but this was minimal compared to the disease progression seen with the wild-type mice, where the majority were deceased by day 365 (removal of wild-type mice for CFU determination was not performed to avoid impacting the survival curve). *M. tuberculosis* dissemination was

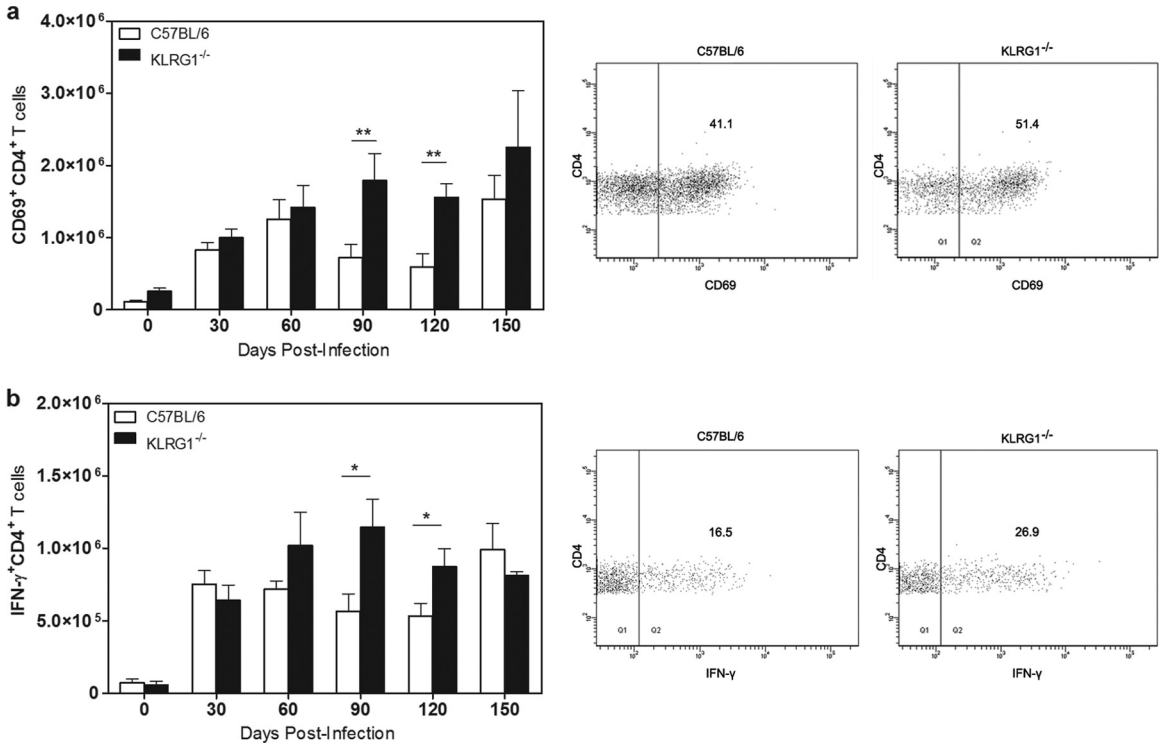

FIG 4 Phenotype of KLRG1$^{-/-}$ pulmonary CD4$^+$ T cells. Wild-type and KLRG1$^{-/-}$ C57BL/6 mice were infected with *M. tuberculosis*. At various time points postinfection, groups of mice were sacrificed and lungs removed and processed for analysis by flow cytometry. (a) Absolute numbers of CD69$^+$ CD4$^+$ T cells, with representative flow plots at day 90 postinfection. (b) IFN-γ$^+$ CD4$^+$ T cells after a 4-h incubation with anti-CD3, anti-CD28, and GolgiSTOP export blocker, with representative flow plots at day 90 postinfection. Data are representative of the results of two independent experiments with 5 mice per group per time point. *, $P < 0.05$; **, $P < 0.01$; ***, $P < 0.001$ (as obtained by Student's *t* test).

not significantly altered, as changes in splenic CFU between wild-type and KLRG1$^{-/-}$ mice were moderate and evident only at day 150 postinfection (Fig. 1c). Therefore, the considerable extension of survival following *M. tuberculosis* infection in KLRG1$^{-/-}$ mice was not associated with reduced dissemination of infection to the spleen or altered granuloma formation but was instead linked to a significant reduction in pulmonary CFU throughout the course of *M. tuberculosis* infection.

To verify that the results obtained with KLRG1$^{-/-}$ mice were not a consequence of subtle genetic variations between the KLRG1$^{-/-}$ colony (Germany) and the wild-type colony (The Jackson Laboratory), a control experiment was performed using KLRG1$^{+/-}$ and KLRG1$^{-/-}$ offspring mice from heterozygous breeding. Similar to the parent KLRG1$^{-/-}$ mice, our hybrid KLRG1$^{-/-}$ mice had significantly lower pulmonary CFU than wild-type and KLRG1$^{+/-}$ mice at day 120 postinfection (Fig. 1d). All together, these data demonstrate that KLRG1$^{-/-}$ mice have significantly extended survival after *M. tuberculosis* infection associated with reduced pulmonary CFU, demonstrating that KLRG1 expression has a functional role *in vivo* during *M. tuberculosis* infection.

KLRG1$^{-/-}$ mice have significantly enhanced CD4$^+$ T cell responses to *M. tuberculosis*. We hypothesized that the reduction in CFU and extended survival of KLRG1$^{-/-}$ mice were direct consequences of altered CD8$^+$ T cell function, as previously demonstrated in viral models (24, 25). Instead, we observed no change in CD8$^+$ T cell numbers (Fig. 3a), phenotype (not shown), or function (not shown) throughout *M. tuberculosis* infection, with the exception of a transient increase in perforin/granzyme B expression at day 90 only (Fig. 3c to f). Contrary to our expectations, KLRG1$^{-/-}$ mice sustained a higher level of total CD4$^+$ T cells than wild-type mice between days 90 and 120 of infection (Fig. 3b). Further analysis by flow cytometry revealed that more CD4$^+$ T cells from KLRG1$^{-/-}$ mice expressed the early activation marker CD69 (Fig. 4a) and were capable of secreting IFN-γ after *ex vivo* T cell receptor (TcR) stimulation (Fig. 4b) during chronic infection. After 48 h of culture with *M. tuberculosis* culture filtrate protein (CFP), CD4$^+$ T cells from KLRG1$^{-/-}$ mice produced significantly more *M. tuberculosis*-specific IFN-γ (Fig. 5a) and TNF (Fig. 5b) than those from wild-type mice during chronic infection. Since the cytokine assays were normalized to cell number, this, together with the intracellular staining results (Fig. 4b), suggests that KLRG1 deficiency has the most impact on T_h1 responses after day 60 of *M. tuberculosis* infection. Our data also indicate that CD4$^+$ T cells and not CD8$^+$ T cells were most affected by the absence of KLRG1 during *M. tuberculosis* infection.

Previous work has indicated that KLRG1 may be responsible for controlling antigen-induced proliferation of T cells during infection (4). Therefore, we examined the proliferation of CD4$^+$ (Fig. 5c) and CD8$^+$ (Fig. 5d) T cells between days 90 and 120 of *M. tuberculosis* infection by *in vivo* BrdU incorporation and saw no significant differences between wild-type and KLRG1$^{-/-}$ mice. This indicates that removal of KLRG1 does not alter the proliferative capability of C57BL/6 CD4$^+$ T cells but instead fundamentally enhances their activation through

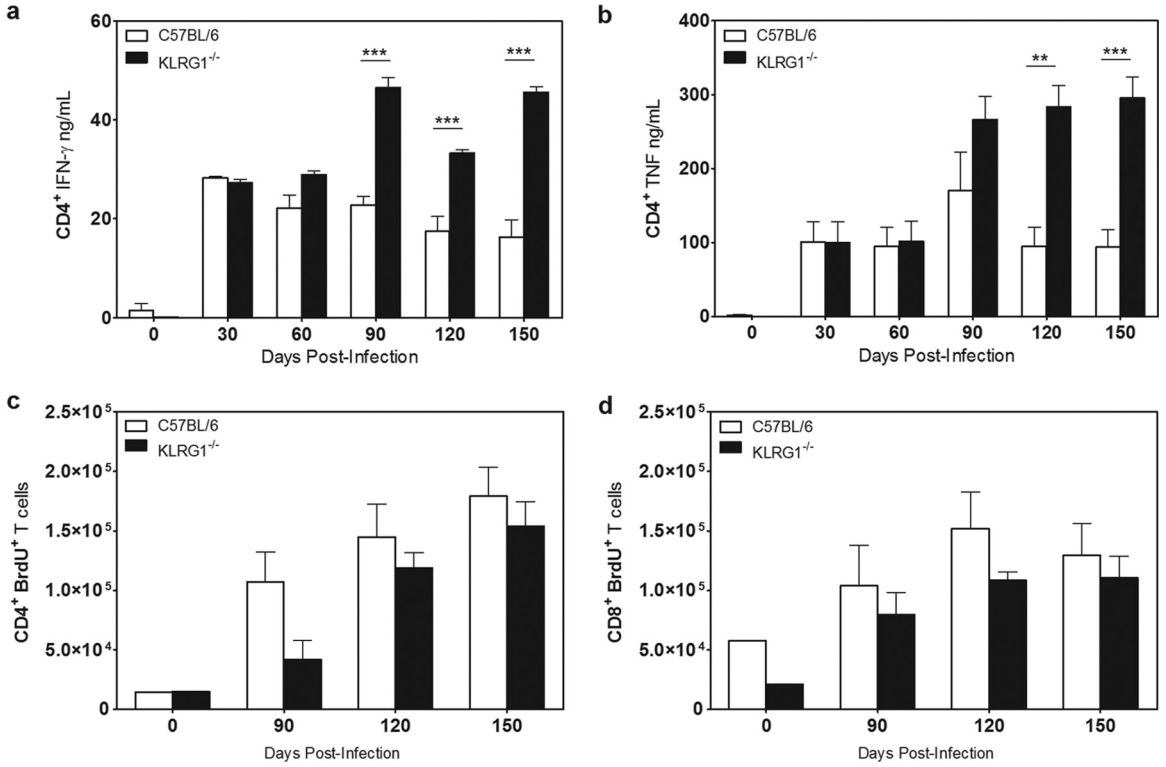

FIG 5 Protective capacity of pulmonary T cells of KLRG1$^{-/-}$ mice. Wild-type and KLRG1$^{-/-}$ C57BL/6 mice were infected with *M. tuberculosis*. At various time points postinfection, groups of mice were sacrificed and lungs removed and processed for analysis by flow cytometry. Using magnetic beads, CD4$^+$ T cells were purified and cultured with *M. tuberculosis* CFP for 48 h. (a and b) The production of IFN-γ (a) or TNF (b) was quantified by ELISA. Data are representative of the results of two independent experiments with 5 mice per group per time point. At 24 h prior to necropsy, mice were injected with BrdU. (c and d) Absolute numbers of BrdU$^+$ CD4$^+$ (c) or CD8$^+$ (d) T cells as determined by flow cytometry. Data are representative of the results of one experiment with 5 mice per group per time point. *, $P < 0.05$; **, $P < 0.01$; ***, $P < 0.001$ (as obtained by Student's *t* test).

the TcR and their ability to secrete proinflammatory cytokines during chronic infection.

Analysis of NK 1.1$^+$ cells at early time points (day 9 and day 20) showed a significant increase in the number of NK cells (NK1.1$^+$/CD3^{neg}) at day 20 post-*M. tuberculosis* infection in the lungs of KLRG1$^{-/-}$ mice relative to wild-type controls (Fig. 6a) but not in the capacity to produce IFN-γ to mitogen stimulation (Fig. 6b). No differences in NK cell proportions or absolute numbers were observed in the spleen at the time points analyzed (not shown). No significant differences in the absolute numbers (Fig. 6c) or proportions (not shown) of NK T (NKT) cells (NK1.1$^+$/CD3$^+$) or IFN-γ-producing NKT cells (Fig. 6d) were observed in the lung or spleen, although a reduced proportion of IFN-γ-producing NKT cells was observed in KLRG1$^{-/-}$ mice (Fig. 6e). Although we observed subtle differences in NK and NKT cell numbers and function between KLRG1$^{-/-}$ and wild-type mice during the first 3 weeks of *M. tuberculosis* infection, such alterations were unable to modify short-term control of *M. tuberculosis* infection.

CD4$^+$ FoxP3$^+$ T regulatory cells have also been shown to express KLRG1 (26), and therefore we analyzed the differences in the proportions of FoxP3$^+$ CD4$^+$ T cells between wild-type and KLRG1$^{-/-}$ mice at days 9 and 20 after *M. tuberculosis* infection. We observed no significant difference in the proportions or absolute numbers of FoxP3-expressing CD4$^+$ T cells in the spleen or lung of wild-type and KLRG1$^{-/-}$ mice (not shown).

KLRG1 expression on wild-type T cells during *M. tuberculosis* infection. To more fully understand when KLRG1 may be important during *M. tuberculosis* infection, we characterized the dynamics of KLRG1 expression on T cells from wild-type C57BL/6 mice. *M. tuberculosis* infection induced the expression of KLRG1 on both CD4$^+$ and CD8$^+$ T cells throughout infection (Fig. 7a and b). In contrast to CD8$^+$ T cells (Fig. 7b), which showed a consistent proportion of KLRG1$^+$ cells, the number of KLRG1$^+$ CD4$^+$ T cells was subsequently reduced around day 90 of infection (Fig. 7a). These data reaffirm that CD8$^+$ T cells are not significantly affected by KLRG1 during *M. tuberculosis* infection and suggest that KLRG1$^+$ CD4$^+$ T cells may be deleted at day 90, shifting the pulmonary CD4$^+$ T cell repertoire to predominantly KLRG1^{neg} (Fig. 7c). Since KLRG1$^{-/-}$ mice had more activated pulmonary CD4$^+$ T cells and were subsequently more protected during chronic infection, we examined the differences in expression of CD69 (indicative of antigen-specific activation) between KLRG1$^+$ and KLRG1^{neg} CD4$^+$ T cells from *M. tuberculosis*-infected wild-type mice. Significantly more KLRG1^{neg} CD4$^+$ T cells expressed CD69 throughout *M. tuberculosis* infection (Fig. 7d). Together, these data demonstrate that the number of pulmonary CD4$^+$ T cells expressing KLRG1 is not constant throughout *M. tuberculosis* infection and match previous findings (13) that few KLRG1$^+$ CD4$^+$ T cells are activated during *M. tuberculosis* infection.

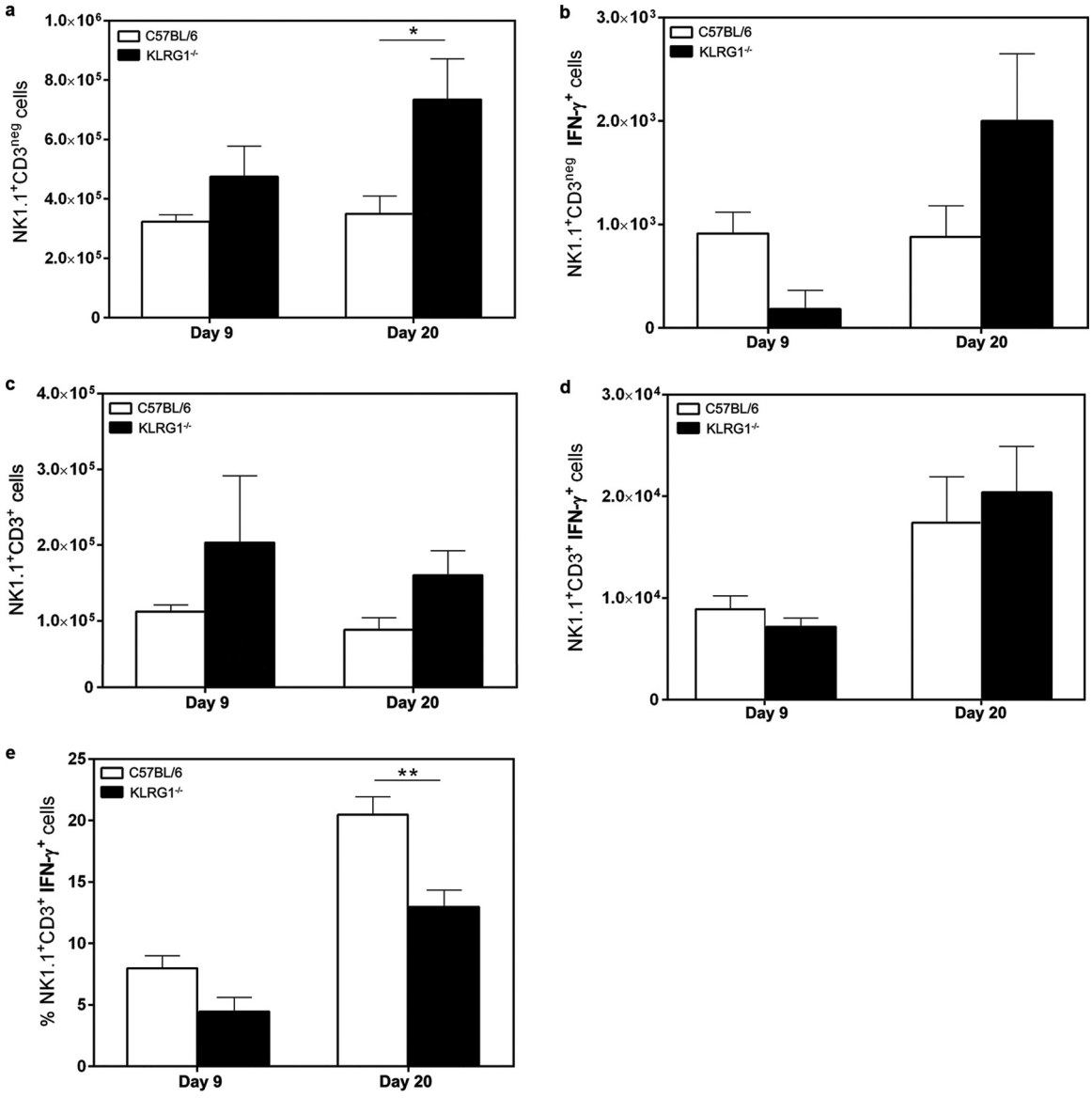

FIG 6 Pulmonary NK/NKT cell composition of KLRG1$^{-/-}$ mice. Wild-type and KLRG1$^{-/-}$ C57BL/6 mice were infected with *M. tuberculosis*. At various time points postinfection, groups of mice were sacrificed and lungs removed and processed for analysis by flow cytometry. Absolute numbers of NK1.1$^+$ CD3^{neg} cells (a), IFN-γ$^+$ NK1.1$^+$ CD3^{neg} cells (b), NK1.1$^+$ CD3$^+$ T cells (c), and IFN-γ$^+$ NK1.1$^+$ CD3$^+$ T cells (d) or proportions of IFN-γ$^+$ NK1.1$^+$ CD3$^+$ T cells (e) as determined by flow cytometry are indicated. IFN-γ$^+$ cell numbers were determined by intracellular staining after a 4-h incubation with ConA and GolgiSTOP export blocker. Data are representative of the results of one experiment with 5 mice per group per time point. *, $P < 0.05$; **, $P < 0.01$; ***, $P < 0.001$ (as obtained by Student's *t* test).

DISCUSSION

Our work is the first demonstration of an *in vivo* consequence of KLRG1 deficiency during infection and provides clear evidence that KLRG1 is more than a marker of terminal differentiation. The absence of KLRG1 leads to decreased pulmonary CFU and significantly extended survival after *M. tuberculosis* infection, and contrary to our expectations, we have demonstrated that CD8$^+$ T cells are not significantly affected by the presence of KLRG1. KLRG1$^{-/-}$ mice maintained high numbers of activated CD4$^+$ T cells during chronic *M. tuberculosis* infection, leading to increased pulmonary IFN-γ levels compared to those seen with wild-type mice. We have also shown that in wild-type mice, activated (CD69$^+$) KLRG1^{neg} CD4$^+$ T cells were more abundant in the lung than KLRG1$^+$ CD4$^+$ T cells during *M. tuberculosis* infection. It is possible that CD4$^+$ T cells are most affected by KLRG1 during *M. tuberculosis* infection, because *M. tuberculosis* has been shown to decrease MHC class II expression and function on macrophages (27–29) and KLRG1 can inhibit suboptimal TcR signaling (30).

Our studies suggest that day 90 post-*M. tuberculosis* infection is a critical time when wild-type mice lose some protective capacity, resulting in a moderate increase in *M. tuberculosis* CFU in the lung, while KLRG1$^{-/-}$ mice are able to exert a continued control of infection. This suggests that a significant biological change occurs in C57BL/6 mice around day 90 postinfection, and that KLRG1$^{-/-}$ mice are refractory or potentially further stimulated by this change. At day 90 postinfection, the inflammatory envi-

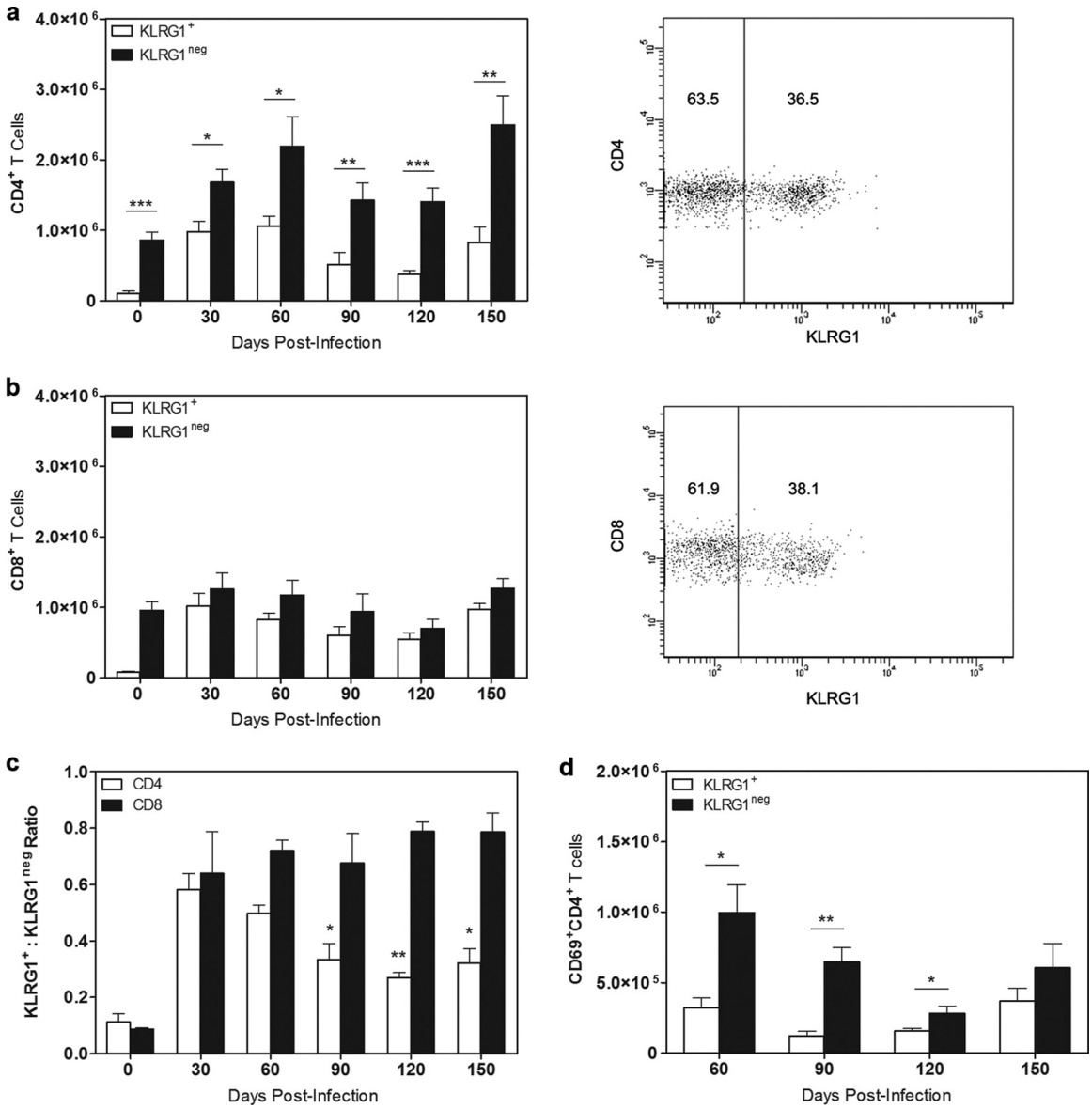

FIG 7 Pulmonary composition of KLRG1$^+$ or KLRG1^{neg} T cells. Wild-type C57BL/6 mice were infected with *M. tuberculosis*. At various time points postinfection, lungs were obtained and processed for analysis. (a and b) Absolute numbers of KLRG1$^{+/neg}$ CD3$^+$ CD4$^+$ T cells (a) or CD3$^+$ CD8$^+$ T cells (b) with representative flow plots at day 150. (c) Ratio of KLRG1$^+$ to KLRG1^{neg} T cells. Statistics represent comparisons of the CD4$^+$ T cell ratio at day 30 to the ratio at day 60, 90, 120, or 150. (d) Absolute numbers of KLRG1$^{+/neg}$ CD3$^+$ CD4$^+$ T cells expressing CD69. Data are representative of the results of two independent experiments with 4 mice per group per time point. *, $P < 0.05$; **, $P < 0.01$; ***, $P < 0.001$ (as obtained by Student's *t* test).

ronment of the lung or the vascularization of *M. tuberculosis* granulomas may change, leading to an increase in the level of available E-cadherin. We also observed that between day 90 and day 120 postinfection, the total number of wild-type CD4$^+$ T cells (but not CD8$^+$ T cells) dropped significantly. It is possible that alterations within the lung at day 90 led to deletion of KLRG1$^+$ CD4$^+$ T cells, thus lowering the overall T_h1 response and affording *M. tuberculosis* a survival advantage in wild-type mice. Similarly, we have demonstrated that KLRG1 does not actively restrict proliferation but serves only to regulate T_h1 effector function during *M. tuberculosis* infection. Indeed, previous work has demonstrated that KLRG1 indirectly affects proliferation by impairing Akt phosphorylation, leading to defective induction of cyclin D and E and no reduction in cyclin inhibitor p27 expression (10). Other studies have demonstrated that KLRG1 restricted the production of the transcriptional repressor Bmi-1 (31), required to maintain proliferation and prevent cell senescence (32–35). KLRG1$^+$ T cells did not induce Bmi-1 after TcR ligation compared to KLRG1^{neg} T cells (31), suggesting that KLRG1$^{-/-}$ T cells are capable of resisting senescence and maintaining normal Akt signaling throughout *M. tuberculosis* infection.

Together, these data provide much-needed insight into the dynamics of protective T cell responses during chronic *M. tuberculosis* infection and demonstrate that KLRG1 expression has a significant impact on the course of disease. We have shown that KLRG1$^{-/-}$ mice were able to survive approximately 35% longer

after *M. tuberculosis* infection and maintained a low level of pulmonary *M. tuberculosis* CFU throughout chronic infection. In contrast to previous viral studies, we have demonstrated that $CD4^+$ T cells were most affected by KLRG1 expression during *M. tuberculosis* infection. Our work provides clear evidence that T cell responses naturally degrade over the course of murine *M. tuberculosis* infection, and that KLRG1 participates in this process. We believe that these findings have important clinical relevance, as the addition of KLRG1 blocking antibody to current treatment regimens could ensure the maintenance of optimal T cell responses, thereby significantly shortening the time required to cure tuberculosis.

ACKNOWLEDGMENTS

Histology services were performed by The Ohio State University's College of Veterinary Medicine, Department of Veterinary Biosciences. The following reagent was obtained through BEI Resources, NIAID, NIH: *Mycobacterium tuberculosis*, strain CDC1551, culture filtrate proteins, NR-14826.

This publication was made possible by grant R01 AI-064522 from NIAID, NIH (J.T.), and by the DFG (SFB620, TP B2) (H.P.).

REFERENCES

1. **Blaser C, Kaufmann M, Pircher H.** 1998. Virus-activated CD8 T cells and lymphokine-activated NK cells express the mast cell function-associated antigen, an inhibitory C-type lectin. J. Immunol. **161**:6451–6454.
2. **Voehringer D, Blaser C, Brawand P, Raulet DH, Hanke T, Pircher H.** 2001. Viral infections induce abundant numbers of senescent CD8 T cells. J. Immunol. **167**:4838–4843.
3. **Hanke T, Corral L, Vance RE, Raulet DH.** 1998. 2F1 antigen, the mouse homolog of the rat "mast cell function-associated antigen", is a lectin-like type II transmembrane receptor expressed by natural killer cells. Eur. J. Immunol. **28**:4409–4417.
4. **Gründemann C, Bauer M, Schweier O, von Oppen N, Lassing U, Saudan P, Becker KF, Karp K, Hanke T, Bachmann MF, Pircher H.** 2006. Cutting edge: identification of E-cadherin as a ligand for the murine killer cell lectin-like receptor G1. J. Immunol. **176**:1311–1315.
5. **Ito M, Maruyama T, Saito N, Koganei S, Yamamoto K, Matsumoto N.** 2006. Killer cell lectin-like receptor G1 binds three members of the classical cadherin family to inhibit NK cell cytotoxicity. J. Exp. Med. **203**:289–295.
6. **Li Y, Hofmann M, Wang Q, Teng L, Chlewicki LK, Pircher H, Mariuzza RA.** 2009. Structure of natural killer cell receptor KLRG1 bound to E-cadherin reveals basis for MHC-independent missing self recognition. Immunity **31**:35–46.
7. **Gründemann C, Schwartzkopff S, Koschella M, Schweier O, Peters C, Voehringer D, Pircher H.** 2010. The NK receptor KLRG1 is dispensable for virus-induced NK and $CD8^+$ T-cell differentiation and function in vivo. Eur. J. Immunol. **40**:1303–1314.
8. **Rosshart S, Hofmann M, Schweier O, Pfaff AK, Yoshimoto K, Takeuchi T, Molnar E, Schamel WW, Pircher H.** 2008. Interaction of KLRG1 with E-cadherin: new functional and structural insights. Eur. J. Immunol. **38**:3354–3364.
9. **Schwartzkopff S, Grundemann C, Schweier O, Rosshart S, Karjalainen KE, Becker KF, Pircher H.** 2007. Tumor-associated E-cadherin mutations affect binding to the killer cell lectin-like receptor G1 in humans. J. Immunol. **179**:1022–1029.
10. **Henson SM, Franzese O, Macaulay R, Libri V, Azevedo RI, Kiani-Alikhan S, Plunkett FJ, Masters JE, Jackson S, Griffiths SJ, Pircher HP, Soares MV, Akbar AN.** 2009. KLRG1 signaling induces defective Akt (ser473) phosphorylation and proliferative dysfunction of highly differentiated $CD8^+$ T cells. Blood **113**:6619–6628.
11. **Robbins SH, Nguyen KB, Takahashi N, Mikayama T, Biron CA, Brossay L.** 2002. Cutting edge: inhibitory functions of the killer cell lectin-like receptor G1 molecule during the activation of mouse NK cells. J. Immunol. **168**:2585–2589.
12. **Henao-Tamayo M, Irwin SM, Shang S, Ordway D, Orme IM.** 2011. T lymphocyte surface expression of exhaustion markers as biomarkers of the efficacy of chemotherapy for tuberculosis. Tuberculosis (Edinb) **91**:308–313.
13. **Reiley WW, Shafiani S, Wittmer ST, Tucker-Heard G, Moon JJ, Jenkins MK, Urdahl KB, Winslow GM, Woodland DL.** 2010. Distinct functions of antigen-specific CD4 T cells during murine Mycobacterium tuberculosis infection. Proc. Natl. Acad. Sci. U. S. A. **107**:19408–19413.
14. **Bengsch B, Seigel B, Ruhl M, Timm J, Kuntz M, Blum HE, Pircher H, Thimme R.** 2010. Coexpression of PD-1, 2B4, CD160 and KLRG1 on exhausted HCV-specific $CD8^+$ T cells is linked to antigen recognition and T cell differentiation. PLoS Pathog. **6**:e1000947. doi:10.1371/journal.ppat.1000947.
15. **Vesosky B, Flaherty DK, Turner J.** 2006. Th1 cytokines facilitate CD8-T-cell-mediated early resistance to infection with Mycobacterium tuberculosis in old mice. Infect. Immun. **74**:3314–3324.
16. **Beamer GL, Flaherty DK, Vesosky B, Turner J.** 2008. Peripheral blood gamma interferon release assays predict lung responses and Mycobacterium tuberculosis disease outcome in mice. Clin. Vaccine Immunol. **15**:474–483.
17. **Beamer GL, Flaherty DK, Assogba BD, Stromberg P, Gonzalez-Juarrero M, de Waal Malefyt R, Vesosky B, Turner J.** 2008. Interleukin-10 promotes Mycobacterium tuberculosis disease progression in CBA/J mice. J. Immunol. **181**:5545–5550.
18. **Rottinghaus EK, Vesosky B, Turner J.** 2009. Interleukin-12 is sufficient to promote antigen-independent interferon-gamma production by CD8 T cells in old mice. Immunology **128**:e679–e690.
19. **Vesosky B, Rottinghaus EK, Stromberg P, Turner J, Beamer G.** 2010. CCL5 participates in early protection against Mycobacterium tuberculosis. J. Leukoc. Biol. **87**:1153–1165.
20. **Kang DD, Lin Y, Moreno JR, Randall TD, Khader SA.** 2011. Profiling early lung immune responses in the mouse model of tuberculosis. PLoS One **6**:e16161. doi:10.1371/journal.pone.0016161.
21. **Medina E, North RJ.** 1998. Resistance ranking of some common inbred mouse strains to Mycobacterium tuberculosis and relationship to major histocompatibility complex haplotype and Nramp1 genotype. Immunology **93**:270–274.
22. **Russell-Goldman E, Xu J, Wang X, Chan J, Tufariello JM.** 2008. A Mycobacterium tuberculosis Rpf double-knockout strain exhibits profound defects in reactivation from chronic tuberculosis and innate immunity phenotypes. Infect. Immun. **76**:4269–4281.
23. **Khader SA, Pearl JE, Sakamoto K, Gilmartin L, Bell GK, Jelley-Gibbs DM, Ghilardi N, deSauvage F, Cooper AM.** 2005. IL-23 compensates for the absence of IL-12p70 and is essential for the IL-17 response during tuberculosis but is dispensable for protection and antigen-specific IFN-gamma responses if IL-12p70 is available. J. Immunol. **175**:788–795.
24. **Bengsch B, Spangenberg HC, Kersting N, Neumann-Haefelin C, Panther E, von Weizsacker F, Blum HE, Pircher H, Thimme R.** 2007. Analysis of CD127 and KLRG1 expression on hepatitis C virus-specific $CD8^+$ T cells reveals the existence of different memory T-cell subsets in the peripheral blood and liver. J. Virol. **81**:945–953.
25. **Thimme R, Appay V, Koschella M, Panther E, Roth E, Hislop AD, Rickinson AB, Rowland-Jones SL, Blum HE, Pircher H.** 2005. Increased expression of the NK cell receptor KLRG1 by virus-specific CD8 T cells during persistent antigen stimulation. J. Virol. **79**:12112–12116.
26. **Beyersdorf N, Ding X, Tietze JK, Hanke T.** 2007. Characterization of mouse CD4 T cell subsets defined by expression of KLRG1. Eur. J. Immunol. **37**:3445–3454.
27. **Gehring AJ, Dobos KM, Belisle JT, Harding CV, Boom WH.** 2004. Mycobacterium tuberculosis LprG (Rv1411c): a novel TLR-2 ligand that inhibits human macrophage class II MHC antigen processing. J. Immunol. **173**:2660–2668.
28. **Noss EH, Harding CV, Boom WH.** 2000. Mycobacterium tuberculosis inhibits MHC class II antigen processing in murine bone marrow macrophages. Cell Immunol. **201**:63–74.
29. **Chang ST, Linderman JJ, Kirschner DE.** 2005. Multiple mechanisms allow Mycobacterium tuberculosis to continuously inhibit MHC class II-mediated antigen presentation by macrophages. Proc. Natl. Acad. Sci. U. S. A. **102**:4530–4535.
30. **Tessmer MS, Fugere C, Stevenaert F, Naidenko OV, Chong HJ, Leclercq G, Brossay L.** 2007. KLRG1 binds cadherins and preferentially associates with SHIP-1. Int. Immunol. **19**:391–400.

31. **Heffner M, Fearon DT.** 2007. Loss of T cell receptor-induced Bmi-1 in the KLRG1(+) senescent CD8(+) T lymphocyte. Proc. Natl. Acad. Sci. U. S. A. **104**:13414–13419.
32. **Park IK, Qian D, Kiel M, Becker MW, Pihalja M, Weissman IL, Morrison SJ, Clarke MF.** 2003. Bmi-1 is required for maintenance of adult self-renewing haematopoietic stem cells. Nature **423**:302–305.
33. **Lessard J, Sauvageau G.** 2003. Bmi-1 determines the proliferative capacity of normal and leukaemic stem cells. Nature **423**:255–260.
34. **Molofsky AV, Pardal R, Iwashita T, Park IK, Clarke MF, Morrison SJ.** 2003. Bmi-1 dependence distinguishes neural stem cell self-renewal from progenitor proliferation. Nature **425**:962–967.
35. **van der Lugt NM, Domen J, Linders K, van Roon M, Robanus-Maandag E, te Riele H, van der Valk M, Deschamps J, Sofroniew M, van Lohuizen M.** 1994. Posterior transformation, neurological abnormalities, and severe hematopoietic defects in mice with a targeted deletion of the bmi-1 proto-oncogene. Genes Dev. **8**:757–769.